Thermodynamics of the Interaction between a Hydrophobically Modified Polyelectrolyte and Sodium Dodecyl Sulfate in Aqueous Solution

Guangyue Bai,[†] Luís M. N. B. F. Santos,[†] Marieta Nichifor,[‡,§] António Lopes,[‡] and Margarida Bastos*[,†]

CIQ (UP), Department of Chemistry, Faculty of Sciences, University of Porto, R. Campo Alegre, 687, P-4169-007 Porto, Portugal, Instituto de Tecnologia Química e Biológica (ITQB/UNL), P-2781-901 Oeiras, Portugal, and "Petru Poni" Institute of Macromolecular Chemistry, Iasi, Romania

Received: August 11, 2003; In Final Form: October 10, 2003

The thermodynamics of the interaction between a hydrophobically modified cationic polyelectrolyte and an anionic surfactant (sodium dodecyl sulfate, SDS) has been investigated by microcalorimetry, conductivity, and UV−vis spectrophotometry. The polyelectrolyte employed was a newly synthesized polymer (D40OCT30) based on dextran having pendant *N*-(2-hydroxypropyl)-*N*,*N*-dimethyl-*N*-octylammonium chloride groups randomly distributed along the polymer backbone with a degree of substitution (DS) of 28.1%. The interaction between D40OCT30 and SDS was found to be very strong because of the introduction of ionic and hydrophobic moieties on the backbone of the dextran polymer. The aggregation concentration of polyelectrolyte−SDS complex ($CAC_{complex}$) was derived from the curves of variation of the observed enthalpy, solution conductivity, and optical dispersion with SDS concentrations. The results show that these values obtained from different methods are coincident and increase with D40OCT30 concentration. A mechanism of interaction is proposed and discussed in detail in the text. The total interaction enthalpies were derived from the observed enthalpy curves. The results indicate that the total interaction process is entropy-driven. From the calorimetric and turbidity measurements, the partial phase diagram that describes the dependence of the phase boundary on polymer alkyl side chain concentration is also deduced.

Introduction

In recent years much interest has been focused on interactions between polyelectrolytes and surfactants because of their widespread application in a variety of fields, such as pharmaceuticals, bioscience, water and soil treatment, and important industrial processes.[1−4] Polyelectrolyte/surfactant (PES) systems often have physicochemical characteristics that differ from nonionic polymer/ surfactant systems.[4−11] Recently Nisha et al.[12] have reported the complex behavior of a poly(ethylene glycol)-based cationic random copolymer/sodium dodecyl sulfate (SDS) system, which gives deeper insight into macromolecular architecture, micellar microcontainers, and drug and gene delivery research.

Considerable efforts have been made to understand the unusual characteristics of various PES systems, mainly those involving rheological and phase behavior,[13−20] microstructure,[7,8,12,21] the molecular self-assembling process, and the mechanism of interaction.[22−36] Many advanced techniques, such as small-angle neutron scattering (SANS)[11,8] and neutron reflection,[32,33] small-angle X-ray scattering (SAXS),[7,8,21] fluorescence methods,[5,12,14] NMR,[27,36] and dynamic and static light scattering[25,26] have been successfully employed in these studies. Polyelectrolyte−surfactant complexes (PESC) can form interesting three-dimensional supramolecular structures in aqueous solution.[7,8] Yeh et al.[7] showed that there exists a highly ordered hexagonal supramolecular structure for the complex of the cationic gel of poly(diallyldimethylammonium chloride) and SDS at an SDS concentration below the critical micelle concentration (cmc). The surfactant ions become more concentrated in the charged network, resulting in the formation of micelle-like aggregates. A desired property of PESC can be obtained by macromolecular architecture.[12] Currently, some investigated hydrophobically modified polyelectrolytes (HMPE) are based on hydrophobic modification of the nonionic polymer or polyelectrolyte precursors. The interaction of the HMPE with the surfactant often generates a variety of unusual properties with a more specific pattern than their unmodified relatives.[10,13,17,36]

It is now well-known that oppositely charged PES systems have a typical phase behavior. In general, a single phase appears in low and high surfactant concentration ranges, and phase separation occurs close to charge neutralization.[13−20] Such behavior is dominated by the change of surfactant concentration and depends on different types of intramolecular and intermolecular interactions in the system, which are generated by the introduction of ionic and hydrophobic moieties, the degree of substitution, charge density, flexibility of the polyelectrolyte backbone, and the surfactant headgroup size and charge, tail group structure, and so forth.[9,28,29] To a large extent the association between polyelectrolytes and surfactants in the bulk solution is governed by a subtle balance of hydrophilic, hydrophobic, and electrostatic interactions. A widely accepted model of the interaction between polyelectrolytes and surfactants is that surfactant molecules adsorb to polyelectrolyte chains as micelle-like aggregates.[14,17] Recently, Mészáros et al. have proposed a mechanism for the hyperbranched polyethyleneimine

* Author to whom correspondence should be addressed. Fax: +351−22−6082959. E-mail: mbastos@fc.up.pt.
[†] University of Porto.
[‡] Instituto de Tecnologia Química e Biológica.
[§] "Petru Poni" Institute of Macromolecular Chemistry.

10.1021/jp036377j CCC: $27.50
Published on Web 12/09/2003

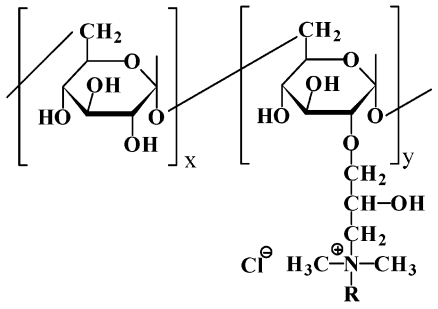

Figure 1. Chemical structure of the cationic polyelectrolyte (D40OCT30) obtained by hydrophobic modification of dextran (R = CH_3 $(CH_2)_7$; degree of substitution is 28.1 mol%).

(PEI)−SDS interaction that differs from the general characteristics of the oppositely charged linear polyelectrolytes and surfactants.[34] Hydrophobically modified polyelectrolytes can associate even with surfactants of the same charge[10,36,37] in which the strongly hydrophobic interaction overcomes the electrostatic repulsion between the charged groups of the polymer and surfactant ionic heads. More detailed thermodynamic information about polymer−surfactant interactions will provide a better understanding of their mechanism. However, reports concerning the thermodynamics of the interaction of a polyelectrolyte with an oppositely charged surfactant are relatively scarce. The determination of the binding isotherm is very important in order to quantify the interactions. Different methods have been used so far for this purpose, such as equilibrium dialysis, membrane selective electrodes for ionic surfactants, and conductivity measurements.[9,11,29,34] Microcalorimetry can provide detailed information on the interactions and thus reveal complex patterns in the interaction between a polymer and a surfactant. In particular, it presents distinct advantages by characterizing both the critical aggregation concentration and the energetics of various interactions and by identifying factors and driving forces that govern the interactions in these systems.[9,11,38−43] Most publications are focused on nonionic polymer/surfactant systems, whereas for polyelectrolyte/surfactant systems there are only a few reports of calorimetric measurements.[9,11,43]

In the present work we have investigated the interaction between a hydrophobically modified cationic polyelectrolyte and SDS by microcalorimetry, conductivity, and UV−vis spectrophotometry. We have studied a newly synthesized polymer (D40OCT30) based on dextran having pendant *N*-(2-hydroxypropyl)-*N*,*N*-dimethyl-*N*-octylammonium chloride groups randomly distributed along the polymer backbone. Each pendant group can be considered as a "polar-end-attached" cationic surfactant (Figure 1). Such an amphiphilic polyelectrolyte has physicochemical characteristics that are quite different from its unmodified relatives as a result of the introduction of the ionic and hydrophobic moieties. We have used a precision isothermal titration microcalorimeter to determine not only the cmc and the enthalpy of micellization of the polyelectrolyte but also the aggregation concentration for the polyelectrolyte−SDS complex ($CAC_{complex}$) and the total interaction enthalpy for the D40OCT30/SDS systems, as well as to pinpoint different interaction events. Parallel conductivity and turbidity measurements have been made on the same mixed system for comparison. The effect of the concentrations of surfactant and D40OCT30 on the behavior of the system will be discussed in detail in the following report.

Experimental Methods

Materials. The cationic polymer with pendant quaternary ammonium groups was synthesized by chemical modification of a dextran sample (Sicomed S. A., Bucharest) with a molar mass M_w = 40 000 and M_w/M_n = 1.12, as determined by capillary viscometry and static light scattering in aqueous solution. The detailed procedure for the synthesis of this polymer and other related cationic polysaccharides will be described in a forthcoming paper. According to the synthetic procedure, dextran was dissolved in deionized water, and a mixture of epichlorohydrin and *N*,*N*-dimethyl-*N*-octylamine (both from Aldrich) was added, and the resulting solution was stirred for 6 h at 70 °C. The polymer was recovered from the reaction mixture by precipitation in acetone and was then purified by repeated precipitation and finally by sequential dialysis against 0.1 N HCl and water. Dialysis tubing with a cutoff of 12 000 from Sigma was used for this purpose. Lyophilization of the diluted aqueous solution obtained after dialysis provided the final polymer as a white powder. The chemical structure was proven by ^{1}H NMR (DMSO-d_6, δ = 4.92 (s, 1H, C^1−H), 4.67 (s, 1H, C^4−OH), 4.51 (s, 1H, C^3−OH), 4.20 (s, 1H, C^2−OH), 4.0−3.1 (bm, 6H, C^2−C^6 H), 3.02 (m, 2H, CH_2−OH from propyl), 1.67(bm, 2H, CH_2−N), 1.28 (m, 12 H, CH_2), 0.85 (t, 3H, CH_3)) and elemental analysis. The concentration of amino groups (degree of substitution, DS) was determined from the nitrogen content (elemental analysis) and chloride ion content (potentiometric titration with $AgNO_3$) and was 28.1 mol% (number of amino groups per 100 glucopyranosidic units). DS = 100 $y/(x + y)$, where x and y are the molar fractions of unsubstituted and substituted glucosidic units, respectively. The polyelectrolyte molecule contains 69.4 positive charges per polymer chain.

The polymer belongs to a series of cationic polysaccharides that we are synthesizing and studying and was coded as D40OCT30, where D40 means dextran of M_w 40 000 and OCT30 indicates the degree of substitution with amino groups carrying an octyl chain as R.

SDS (Bethesda Research Laboratories, 99.5%), KCl (Merck), and NaCl (Merck) were used without further purification. All of the solutions were prepared either by weight or volume using water produced by a Milli-Q filtration system and were stabilized at room temperature for 2 days before use.

Isothermal Titration Microcalorimetry (ITC). The microcalorimeter unit used in this work consisted of a twin heat conduction calorimeter with a 3 mL titration cell (ThermoMetric AB, Järfalla, Sweden), a water bath and its controller (built at Lund University, Sweden), and a $7^1/_2$ digit HP nanovoltmeter connected to the calorimetric channel and to the computer. A gold stirrer formed by a paddle and 2 propellers above, as well as a Kel-F turbine, both made at Lund University, Sweden, were used at a stirring speed of 100 rpm. We checked for the quality of stirring and mixing by use of a transparent cell, which was outside of the calorimeter and at the same temperature. The stirring speed was thereafter adjusted, so as to ensure complete dispersion. The instrument was calibrated electrically, using an insertion heater with a precision better than ±0.5%.[44] The calorimetric titration experiments consisted of a series of consecutive additions of concentrated SDS solution into water or concentrated SDS + polymer solutions into polymer solution of the same polymer concentration. The volume of solution or water in the calorimetric vessel was 2.6 mL. The purpose of having polymer in the syringe was to maintain a constant polymer concentration.[11] The titrating solution was automatically added in aliquots of 4.16−8.32 μL from a modified gastight Hamilton syringe through a thin stainless steel capillary until the desired range of concentration had been covered. Each experiment consisted of 42 consecutive injections and was

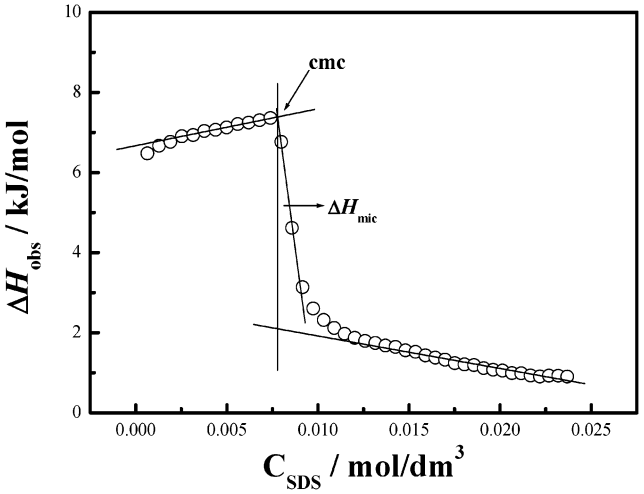

Figure 2. Microcalorimetric titration curve for the dilution of concentrated SDS (0.2M) into water at 308.15K.

repeated at least 3 times. The fast titration procedure was used with a 7 min interval between each injection, and the potential signal was corrected thereafter according to the Tian equation.[45] Data acquisition and syringe pump control were performed through a modified version for ITC of the LABTERMO program.[46] All experiments were performed at 308.15 ± 0.01 K.

Conductivity Measurements. Conductivities for pure SDS solution, pure D40OCT30 solution, and a mixed solution of D40OCT30 and SDS were measured with a CDM210 conductivity meter (CDC641T electrode, France) at 308.15K. The conductivity meter was calibrated with a standard solution of known conductivity (0.1M KCl). The conductivity measurements for the D40OCT30/SDS system were carried out by titrating a concentrated SDS solution containing a known concentration of D40OCT30 into an aqueous solution containing the same amount of D40OCT30. Reference conductivity curves for SDS were also measured, where pure SDS was titrated into water, the conductivity of which was adjusted with NaCl to the initial conductivity of the pure D40OCT30 solution as found in the conditions of each experiment. For all experiments, the conductivity was recorded when its fluctuation was less than 1% in 2 min.

Turbidity Measurements. The turbidity of the D40OCT30/SDS solutions was measured using an 845× UV−vis spectrophotometer at a wavelength of 400 nm in a quartz sample cell with a light path of 10 mm, thermostated at 308.15K with a water bath. The concentrations of the SDS and D40OCT30 solutions were the same as those used for the ITC and conductivity experiments. The measured values of turbidity were corrected with the polymer-free blank and were only recorded after the values became stable (about 2−3 min).

Results and Discussion

Self-Aggregation of Hydrophobically-Modified Polyelectrolyte (D40OCT30). Microcalorimetric curves for the dilution of the surfactant, SDS, and the investigated polyelectrolyte, D40OCT30, are shown in Figures 2 and 3, where the observed enthalpies (ΔH_{obs}) for each injection are plotted against the final concentrations of SDS and D40OCT30 in the calorimetric vessel, respectively. The dilution of a concentrated solution of SDS (Figure 2) was found to be endothermic, with a clear break corresponding to the cmc. As has been discussed previously in the literature,[47] when the final concentration is below the cmc,

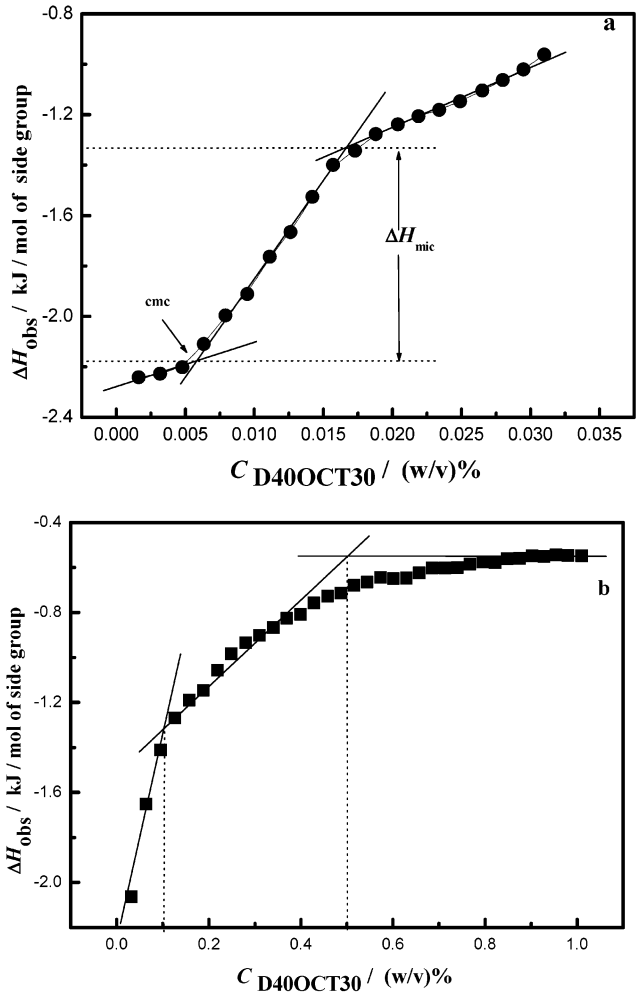

Figure 3. Microcalorimetric titration curves for the dilution of concentrated D40OCT30 into water at 308.15K: (a) 1 (w/v)%; (b) 10-(w/v)%.

the added micelles dissociate into monomers and the monomers are further diluted. When the final concentration is above the cmc, the added micelles are only diluted without dissociation. The enthalpy of micellization (ΔH_{mic}) can therefore be obtained from the difference between the observed enthalpies of the two linear segments of the plots, as calculated at the crossing points. The obtained cmc (7.78 ± 0.02 mM) and ΔH_{mic} (−5.35 ± 0.06 kJ/mol) at 308.15K are in good agreement with literature values.[47]

Microcalorimetric curves for the dilution of concentrated D40OCT30 (1% and 10%) into water are shown in Figure 3. The dilution process is exothermic. In Figure 3a, where 1% D40OCT30 solution is titrated into 2.6 mL of water, the pattern of enthalpy change on dilution is very similar to that of conventional surfactants, as we observe a break corresponding to some kind of deaggregation. Because a number of cationic surfactant-like side chains are grafted onto the hydrophilic polymer backbone, it is possible that micelle-like clusters of side alkyl chains are formed. The intramolecular attractive hydrophobic interaction might overcome the electrostatic repulsive interaction and the energy to bend the polymer backbone. We denote the concentration at which aggregation starts as the cmc of the amphiphilic polyelectrolyte. According to the calculation method referred to previously (Figure 2), the cmc and ΔH_{mic} of D40OCT30 were found to be 0.006 (w/v)% and 0.84 kJ/(mol of side group), respectively. The positive enthalpy change indicates that the intramolecular self-assembly process

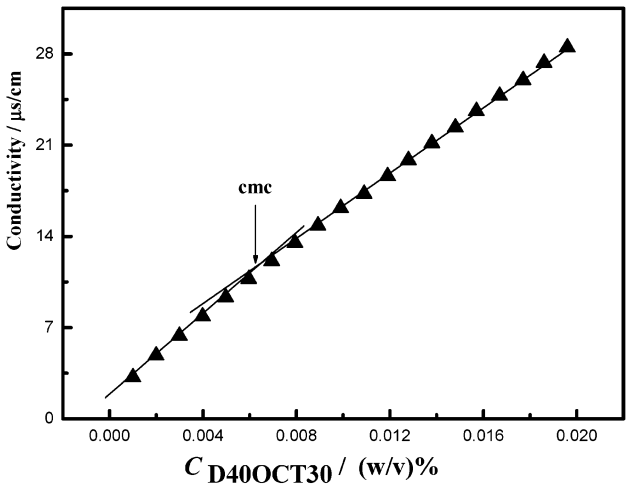

Figure 4. Solution conductivity for the titration of 1% D40OCT30 into pure water at 308.15K.

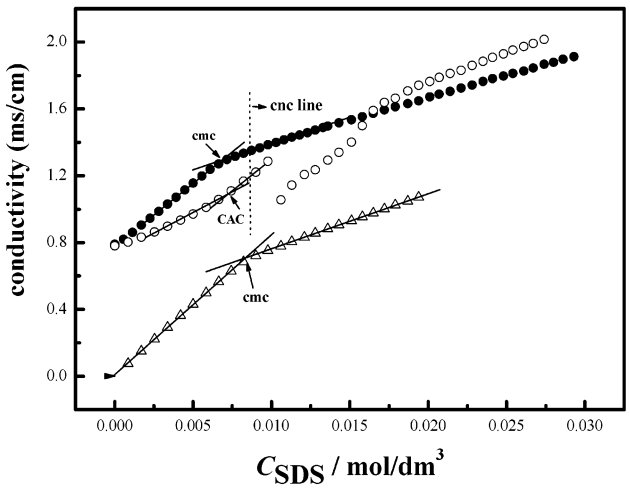

Figure 5. Solution conductivity vs total concentration of SDS (C_{SDS}). Titration of SDS (0.2M) into pure water (△); titration of SDS (0.2M) + polymer (0.75%) into 0.75% polymer solution (○); titration of SDS (0.2M) into NaCl ($c \ll 0.01$ M) solution with the same initial conductivity as that initially measured in pure 0.75% D40OCT30 solution (●).

is entropy-driven at 308.15K. The cmc of D40OCT30 was also obtained by a parallel conductivity measurement. As shown in Figure 4, there is also a break at 0.006% in the conductivity versus concentration curve, corresponding to the cmc determined from the microcalorimetric curve (Figure 3a). Bordi et al.[48] studied the conductivity of polyacrylate aqueous solutions in the semidilute and concentrated regime and observed a similar deviation from a straight line that evidences different concentration regimes.

Figure 3b shows the dilution curve of a 10% D40OCT30 solution titrated into 2.6 mL of water. When the D40OCT30 concentration reaches about 0.1%, the change in ΔH_{obs} with D40OCT30 concentration gradually slows down, eventually approaching a constant ΔH_{obs} value (−0.56 kJ/(mol of side group)) at a polymer concentration above 0.5%. This suggests that as the concentration increases, intermolecular micelle-like clusters form that grow in number and size. It is clearly seen from the curve that the intermolecular self-aggregation is a gradual process, and a beginning point at about 0.1% can be obtained from the intersection point of the tangent lines. This aggregation process can be expected to be gradual as the side groups ($R = CH_3$ $(CH_2)_7$) are not hydrophobic enough for a sharp transition to be observed. For a similar polyelectrolyte, QUATRISOFT LM200, steady-state fluorescence measurements showed that hydrophobic microdomains were formed in aqueous solutions at low concentrations (≪1%).[13] Raju et al.[49] investigated the thermodynamics of micellization of amphiphilic polyelectrolytes, HM-PAMPS, in aqueous solutions by means of ITC. Their observations on the micellization processes of HM-PAMPS are, to some extent, similar to ours, as they obtain a similar shape for the titration curves. Assuredly, ITC is an ideal technique to measure, in the absence of any probe, the cmc and enthalpy of micellization of surfactants as well as those of amphiphilic polyelectrolytes. The fact that we observe intramolecular and intermolecular associations in low and high concentration ranges will be further discussed in the following study on mixtures of D40OCT30 and SDS.

Determination of the Aggregation Concentration of Polyelectrolyte−SDS Complex ($CAC_{complex}$) by Conductivity. The measurement of conductivity is a conventional method to determine the cmc of surfactants, where the cmc values can be obtained from the intersection of the tangent lines before and after a break in conductivity. Similarly, for the D40OCT30−SDS systems, the aggregation concentration of the polyelectrolyte−SDS complex ($CAC_{complex}$) can be derived from the conductivity of the D40OCT30/SDS solution as a function of surfactant concentration, as shown in Figure 5 and summarized in Table 1. For the titration of pure SDS into water, the conductivity below the cmc is due to the sum of the contributions of the free Na^+ and dodecyl sulfate (DS^-) ions. Above the cmc, the rate of increase in conductivity is smaller because micelles have lower mobility than the free DS^- ions and a fraction of the sodium ions are ion-paired with the micelles.[9] For comparison, a reference conductivity curve obtained for the titration of pure SDS into a solution of NaCl is also given in Figure 5, where the initial conductivity of the NaCl solution was adjusted to be the same as that of the pure D40OCT30 solution (0.75%) so that the effect of the ionic strength on the SDS cmc is considered. According to the observed break on the curve, the cmc of SDS is 6.86 mM under this condition, which is lower than that of SDS in the absence of NaCl, as we could expect. In the same figure we also plot the conductivity curve in the presence of D40OCT30 (0.75%), where an obvious break point at 7.26 mM is obtained. Before this point, the conductivity increases linearly as the SDS concentration increases, and it then deviates gradually from the reference curve, which indicates a strong binding of SDS with the polyelectrolyte; thus, the polyelectrolyte−SDS complex is formed. When the SDS concentration reaches the break point, the polyelectrolyte−SDS complex starts to form aggregates. Thus, we can refer to this break point as the aggregation concentration ($CAC_{complex}$) of the polyelectrolyte−SDS complex. After the $CAC_{complex}$ but before the phase separation, the conductivity increases more steeply than before the $CAC_{complex}$, which means that the aggregation process is accompanied by the release of the most of the counterions. At an SDS concentration above the charge neutralization point (cnc), phase separation occurs and the conductivity decreases suddenly, which means that most of the counterions associate with the network structure. At an even higher SDS concentration redissolution occurs, and the release of most of the counterions leads to an increase in conductivity, eventually exceeding that of the SDS reference curve.

From Table 1 we can see that the $CAC_{complex}$ values depend largely on the D40OCT30 concentration, as they are affected mainly by charge neutralization of the polyelectrolyte by SDS and also by the hydrophobic interaction between the alkyl chains of SDS and D40OCT30 and the ionic strength of the media.[5,14]

TABLE 1: $CAC_{complex}$ and $\Delta H_{total\ int}$ Values of the D40OCT30/SDS Systems at 308.15K, the Molar Ratio of SDS to D40OCT30 (n_{SDS}:$n_{D40OCT30}$) at $CAC_{complex}$, and the Charge Neutralization Concentration (cnc) of SDS

$C_{D40OCT30}$ (%)	$CAC_{complex}$ (mM)			$\Delta H_{total\ int}$ (kJ/mol(SDS))	n_{SDS}:$n_{D40OCT30}$ at $CAC_{complex}$	cnc (mM)[b]
	microcalorimetry[a]	conductivity	turbidity			
0.01	0.12	0.1	0.1	19.7	71	0.12
0.025	0.31	0.3	0.3	19.5	70	0.30
0.05	0.62	0.6	0.6	19.4	71	0.61
0.1	1.00	1.0	1.0	19.3	58	1.21
0.25	2.4	2.8	2.5	15.0	54	3.03
0.5	4.8	4.9	4.2	13.0	55	6.05
0.75	7.3	7.3	7.3	10.6	56	9.08
1	9.2	8.8	8.4	10.6	53	12.1

[a] The error is less than 2% in the lower polymer concentration and about 4% above 0.25%. [b] With 69.4 positive charges per D40OCT30 molecule.

The Observed Enthalpy Patterns for D40OCT30/SDS Systems. The calculated enthalpy curves for the titration of concentrated SDS + D40OCT30 into D40OCT30 solutions of different concentrations (0.01−1 (w/v)%) are shown in Figure 6a,b, and the corresponding dilution curves for concentrated SDS solution into water are also included for comparison. These curves have two features: (i) Initially the process is exothermic in the presence of D40OCT30 but endothermic in its absence. (ii) After a variable number of injections (depending on the polymer concentration), there is a change from a large exothermic effect to a small exothermic or endothermic effect, as the surfactant concentration increases at constant D40OCT30 concentrations. The existence of endothermic and exothermic effects, the change in magnitude of the effect as the titration proceeds, and the emergence of a break on the ITC curves give more detailed information about the interaction between the surfactant and the polyelectrolyte.

The calculated enthalpy curves of SDS dilution in the presence of oppositely charged polyelectrolyte are usually more complex than those in the presence of nonionic polymer, because of the electrostatic attractive interaction between oppositely charged groups and the electrostatic repulsive interaction between similarly charged polar headgroups. The value of ΔH_{obs} for each injection, obtained by integration of the observed peak, is plotted in Figure 6a,b against the final concentration of SDS in the calorimetric vessel, in the presence and absence of D40OCT30. From these observed enthalpy curves, the onset points of the break under different polymer concentrations can well define the $CAC_{complex}$ values at which the polyelectrolyte−SDS complex self-assembles into larger aggregates (cross-linking aggregates). In Table 1 we also present the observed $CAC_{complex}$ values, as well as the molar ratio between SDS and D40OCT30 at the $CAC_{complex}$ and the SDS concentration at the cnc. The $CAC_{complex}$ values obtained from microcalorimetry agree with those obtained from conductivity.

In the beginning of the titration we observe positive ΔH_{obs} values for the dilution of SDS into water and negative ΔH_{obs} values in the presence of D40OCT30. This difference suggests that the exothermic effect is caused by strong electrostatic and hydrophobic interactions between SDS and D40OCT30. It is worth noting that the absolute value of the exothermic effect after each injection depends on the initial SDS and polymer concentration and on the SDS molar ratio to polyelectrolyte in the syringe, and thus we cannot compare the exothermic magnitude of the respective curves, but the slope of the line before the break can give us some information. It was found that the slope depends on the polyelectrolyte morphologies in aqueous solution. For higher polymer concentration (above 0.25%, Figure 6a), ΔH_{obs} values are almost constant below the $CAC_{complex}$, but for lower polymer concentration (below 0.1%,

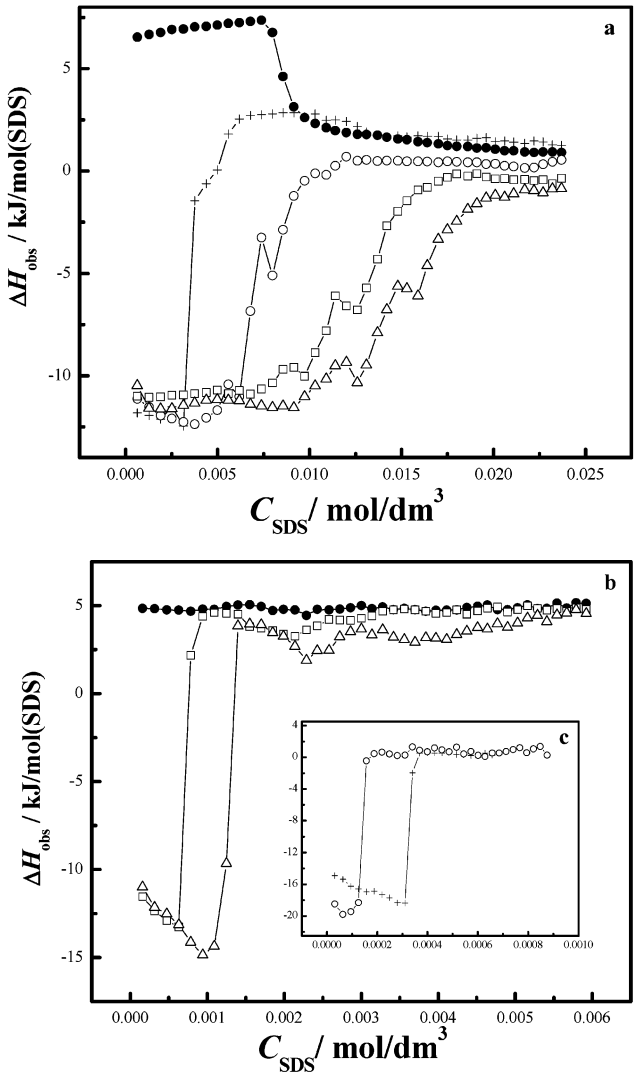

Figure 6. Variation of the observed enthalpy with SDS concentration for the titration of SDS + polymer into polymer aqueous solution. (a) Titration of SDS (0.2M) into pure water (●); titration of SDS + polymer into polymer solutions: 1% (△), 0.75% (□), 0.5% (○), and 0.25% (+). (b) Titration of SDS (0.05M) + polymer into 0.1% (△) and 0.05% (□) polymer solutions, respectively. (c) (inset in part b) Titration of SDS (0.01M) + polymer into 0.025% (+) and 0.01% (○) polymer solutions, respectively.

Figure 6b), negative ΔH_{obs} values increase linearly with increasing SDS concentration. As has been mentioned previously, in the investigated concentration range (0.01−1%) the polyelectrolyte solution already presents some kind of aggregation (i.e., intramolecular and intermolecular aggregates) in the

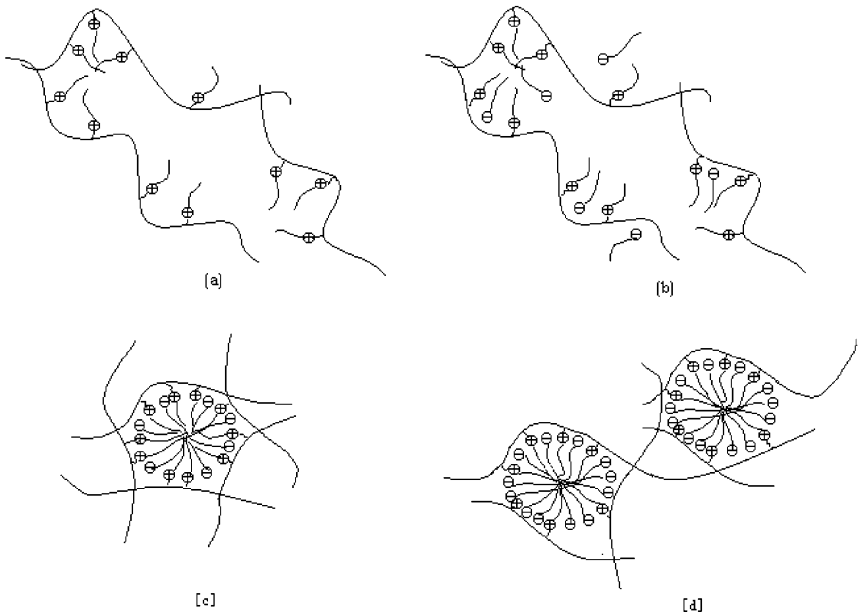

Figure 7. Schematic representation of the association process between D40OCT30 and SDS. (a) D40OCT30 solution in the absence of SDS. (b) Mixed hydrophobic clusters for the polyelectrolyte−SDS complex are formed when the concentration of surfactant is below the $CAC_{complex}$. (c) Mixed micelles for the polyelectrolyte−SDS complex with positive net charges are formed when the concentration of surfactant is above the $CAC_{complex}$ but below the cnc. (d) SDS-rich mixed micelles with negative net charges are formed after redissolution.

absence of SDS, which means that the SDS monomers will interact with the polymer probably forming mixed aggregates. Intramolecular aggregation (<0.1%) is small and not compact, and electrostatic binding of SDS is accompanied by its cooperative self-aggregation, and the size and number of aggregates grow with increasing SDS concentration, which makes the slope negative. At a polymer concentration >0.25% the size of the hydrophobic microdomains formed (intramolecular micelle-like or cross-linking aggregates) is larger and the aggregates are more compact. The electrostatic shield of counterions partly counteracts the attractive electrostatic interaction between the polyelectrolyte and SDS. In both cases the aggregate size cannot change much with increasing SDS concentration, and thus the slope changes only slightly in this range. After the break point, the titration curves in the presence of D40OCT30 change sharply and reach a constant value that is very close to that of pure SDS at low polyelectrolyte concentration, indicating dilution of the SDS micelles. Any differences between the observed curves with and without D40OCT30 must result from strong polyelectrolyte−surfactant interaction, which will be discussed from a proposed mechanism of interaction between D40OCT30 and SDS.

Mechanism of Interaction between D40OCT30 and SDS. As described previously, the patterns of variation of the observed enthalpy with SDS concentration depend on the D40OCT30 concentration. In cases where the D40OCT30 concentrations are above 0.25%, calorimetric curves are more complicated than in those below 0.1%. To understand the thermodynamic processes that each curve reflects, a mechanism of interaction between D40OCT30 and SDS is proposed, with a schematic representation shown in Figure 7. The mechanism is based on the assumption that the surfactant comicellizes with the segment grafted with cationic surfactant-like side chains but does not associate with the unsubstituted segment.[13] The observed enthalpy curve in the presence of 0.75% D40OCT30 was chosen as a detailed representative of these systems for a polymer concentration higher than 0.25%. Five stages can be identified from the titration curve (see Figure 8). The first stage occurs below the $CAC_{complex}$. At this polymer concentration (0.75%)

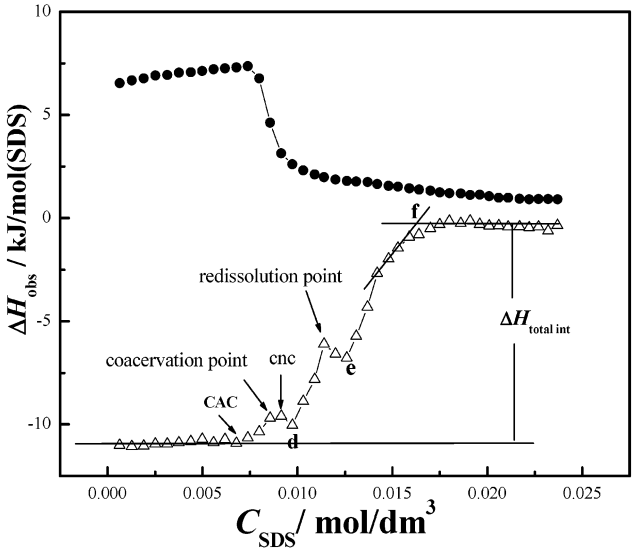

Figure 8. Detailed analytical example in these investigated systems. Titration of SDS (0.2M) into pure water (●); titration of SDS (0.2M) + polymer (0.75%) into 0.75% polymer (△).

the side alkyl chains of the polymer have associated into hydrophobic microdomains before surfactant addition. Accordingly, the SDS monomers can bind with the polyelectrolyte into the microdomains as a result of the strong electrostatic and hydrophobic interactions. Mixed hydrophobic clusters are thus obtained in this concentration range (Figure 7b). At the $CAC_{complex}$, cross-linking aggregates begin to form, with a molar ratio between SDS and D40OCT30 ($n_{SDS}/n_{D40OCT30}$) of 56:1 (see Table 1). When the SDS concentration is above the $CAC_{complex}$ but below the cnc (the second stage), the aggregates increase in number and in size (i.e., aggregation number) and carry a net positive charge almost until charge neutralization ($n_{SDS}/n_{D40OCT30} = 69:1$) is reached (Figure 7c). These mixed micelles are stabilized as a result of the still positive overall charge of the complex and do not separate from the solution. When the SDS concentration is close to the cnc (11.46 mM), the coacervation of D40OCT30−SDS starts to occur (the third

stage). The hydration of the aggregates becomes quite weak, as their hydrophilic shell is broken down as a result of a decreasing net charge.[13] Furthermore, this leads to an increasingly exothermic process within a narrow concentration range because the hydrophobic interaction energy between the side alkyl chains is larger than the hydrated energy of the almost-neutralized headgroups and the hydrophilic polymer backbone. The lowest point (point d) in Figure 8 indicates complete phase separation. The sudden decrease of the conductivity in the liquid phase also indicates that most of the counterions are associated in the network structure. Beyond point d the added SDS reacts with the cross-links of the D40OCT30−SDS at the interface of the two phases and at the same time the concentration of free SDS molecules in the solution increases, as reflected by a new increase in the solution conductivity (Figure 5). On further addition of SDS, the process becomes more exothermic with the formation of SDS-rich mixed micelles (from the redissolution point to point e in Figure 8). The reason for this increase is that the hydrated energy of the increasingly negatively charged mixed micelles is larger than the hydrophobic energy between the alkyl chains. Swelling of the gel occurs, and the mixture gradually becomes a transparent solution, depending on the ratio of SDS to D40OCT30 and the ionic strength of solution (forth stage).[13] This process continues until point f, where the gel dissolves completely to form mixed micelles with net negative charges (Figure 7d). It is possible that some pure SDS micelles are also formed later, especially for mixtures of low D40OCT30 concentration, but no further break is observed in the enthalpy curve. For mixtures with low D40OCT30 concentrations (below 0.1%), the cross-links of the D40OCT30−SDS are not large enough for a clear phase separation and no coacervation point is observed on the microcalorimetric curve (Figure 6b). The solutions are turbid, as observed in optical dispersion experiments (discussed in the following text).

When trying to rationalize the change in morphology from a to b and d (Figure 7), we should keep in mind that the D40OCT30 concentration in the syringe is the same as in the vessel, that is, the polymer concentration is constant throughout the experiment. We can assume that the reaction takes place in two steps: (i) D40OCT30−SDS dissociates to D40OCT30 and SDS, and (ii) SDS monomers associate again with all of the D40OCT30 molecules. For the process from a to b, the equation can be written as follows:

$$m\text{SDS} + (\text{D40OCT 30}) \rightarrow (\text{D40OCT30})(\text{SDS})_{m(\text{complex})} \quad (1)$$

where m is the molar ratio of the complex between D40OCT30 and SDS. Similarly, for the process from a to d, we can write the equation as follows:

$$n\text{SDS} + (\text{D40OCT30}) \rightarrow (\text{D40OCT30})(\text{SDS})_{n(\text{aggregate})} \quad (2)$$

where n ($>m$) is the molar ratio of D40OCT30 to SDS in the aggregates. $(\text{D40OCT30})(\text{SDS})_{m(\text{complex})}$ and $(\text{D40OCT30})(\text{SDS})_{n(\text{aggregate})}$ correspond to the morphologies in Figure 7b and Figure 7d. Accordingly, the total equation for the full titration curve is deduced to be

$$(n-m)\text{SDS} + (\text{D40OCT30})(\text{SDS})_{m(\text{complex})} \rightarrow (\text{D40OCT30})(\text{SDS})_{n(\text{aggregate})} \quad (3)$$

We can define the total interaction enthalpy ($\Delta H_{\text{total int}}$) as corresponding to the process described in eq 3, and it can be calculated from the difference between the two linear segments that occur before and after the steep break. The results listed in Table 1 show that for the D40OCT30/SDS systems, $\Delta H_{\text{total int}}$ is endothermic. The values for $\Delta H_{\text{total int}}$ are approximately the same for the systems with polymer concentrations below 0.1%, but as the polymer concentration increases the values decrease. Such a variation in the $\Delta H_{\text{total int}}$ values gives an important insight into the effect of the polyelectrolyte's microstructure on the polyelectrolyte−surfactant interaction. The result reflects the initial morphologies of pure D40OCT30, that is, the presence of intramolecular or intermolecular polymer self-aggregates. There are four main contributing factors to the total interaction enthalpy: (i) the electrostatic interaction between headgroups of the surfactant and oppositely charged groups of the polyelectrolyte, (ii) the hydrophobic interaction between the alkyl side chains of the polyelectrolyte and the surfactant alkyl chains, (iii) conformational changes of the polyelectrolyte induced by the surfactant, and (iv) the repulsive interaction between the charged groups of the polyelectrolyte before the cnc and between the headgroups of SDS after the cnc. Indeed we cannot get values for the separate effects we can just observe that their balance leads the total interaction enthalpy to endothermic values. This suggests that such an interaction process is entropy-driven.

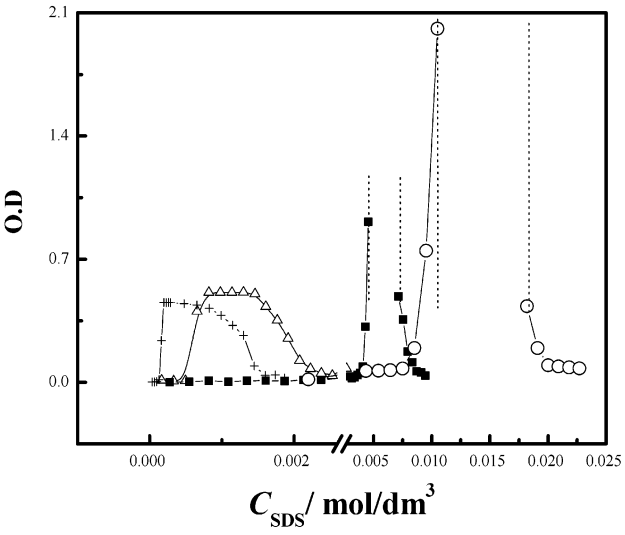

Figure 9. Turbidity (optical dispersion) of mixed solutions of D40OCT30 and SDS as a function of total SDS concentration measured at a wavelength of 400 nm and a temperature of 308.15K. The concentrations of D40OCT30 are 1% (○), 0.5% (■), 0.05% (△), and 0.01% (+).

Turbidity Measurements of Mixtures of D40OCT30 and SDS. Macroscopic phase behavior of polyelectrolyte/surfactant mixtures can be obtained from turbidity measurements. For the D40OCT30/SDS systems with different constant concentrations of D40OCT30, the variation of turbidity as a function of SDS concentration is shown in Figure 9. All of the curves have the following common features: (i) When the SDS concentration is below the $\text{CAC}_{\text{complex}}$ the mixture is transparent, with a single phase. (ii) After the SDS concentration reaches a certain value, the optical dispersion increases steeply with increasing SDS concentration because of the light dispersion (scattering) by large size aggregates. We observed that the SDS concentration at which the sudden increase starts is in agreement with the $\text{CAC}_{\text{complex}}$ as determined by calorimetry and conductivity, indicating that at this point mixed micelles start to form. The $\text{CAC}_{\text{complex}}$ values from the turbidity measurement are also listed in Table 1. (iii) When the SDS concentration is close to the cnc for systems with D40OCT30 concentrations below 0.1%, the turbidity increases without precipitation, which suggests that

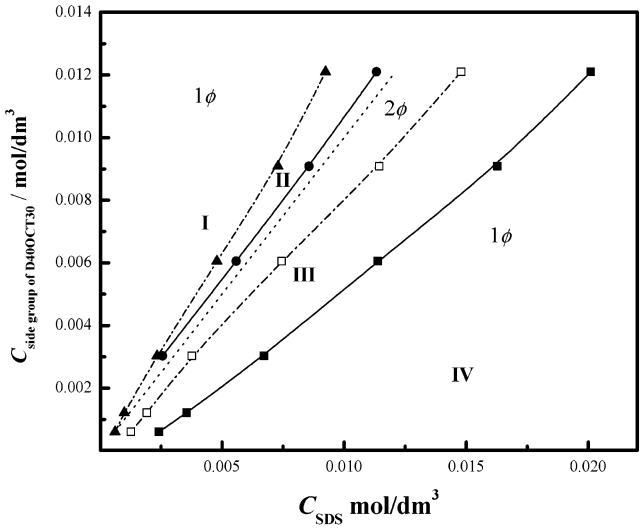

Figure 10. The partial phase diagram of the D40OCT30/SDS systems. (▲) $CAC_{complex}$ line; (●) coacervation line; (···) charge neutralization line (cnc); (□) redissolution line; (■) mixed micelle's line. Region I: liquid phase of the D40OCT30-SDS complex. Region II: stable semitransparent liquid with microstructure as described in Figure 7c. Region III: a two-phase area (D40OCT30-SDS gel and liquid phase). Region IV: liquid phase with microstructure as described in Figure 7d.

more side chain groups of the D40OCT30 molecules associate together in mixed micelles and the cross-linking of the polymer becomes larger. However, when the polymer concentration is above 0.25% and the SDS concentration is close to the cnc, coacervation occurs and an obvious phase separation is observed. For this reason, we see a discontinuity in the dispersion curves. Furthermore, in the SDS concentration range between the $CAC_{complex}$ and phase separation, despite the high turbidity these semitransparent solutions are stable with time. (iv) When the SDS concentration is further increased, the scattering decreases with SDS concentration until it reaches a constant value. Such a decrease in scattering comes from redissolution, which is due to the formation of negatively charged surfaces of mixed micelles. When the hydrophobic side chains of D40OCT30 are saturated with micelles, the excess SDS can probably form free SDS micelles.

Phase Behavior of the D40OCT30/SDS System. Microcalorimetric measurements can provide information on the phase boundaries of some mixed systems, for example nonionic polymer/surfactant systems and anionic/cationic surfactant mixed systems.[42,50] For the present polyelectrolyte/surfactant systems, the $CAC_{complex}$ and the coacervation and redissolution points can be identified from the observed enthalpy change curves (Figure 8). From the calorimetric and turbidity measurements the partial phase diagram that describes the dependence of the phase boundary on concentration of the side groups of the polyelectrolyte is deduced and shown in Figure 10, where four regions are distinguished by these phase boundaries. Region I is below the $CAC_{complex}$ and is a single-phase area (see part b in Figure 7). Region II lies between the $CAC_{complex}$ and the coacervation lines and describes another stable single-phase area where the mixed solution becomes semitransparent (see part c in Figure 7). Regions III is a two-phase area, where coacervation and redissolution processes occur. Region IV corresponds again to a single-phase area (see part d in Figure 7). From the phase diagram, it is clearly seen that the coacervation line is close to the charge neutralization line, which is similar to Guillemet and Piculell's observation on the QUATRISOFT LM200/SDS system.[13] Though calorimetric measurements cannot be used directly to obtain phase morphology, they identify the phase boundaries, unless the enthalpy change from one phase morphology to another is too small to be detected or the variational process is too slow to adapt to titration calorimetry.[50]

Conclusion

A hydrophobically modified cationic polyelectrolyte based on dextran having pendant *N*-(2-hydroxypropyl)-*N*,*N*-dimethyl-*N*-octylammonium chloride groups randomly distributed along the polymer backbone (D40OCT30) can self-associate into intramolecular or intermolecular micelle-like clusters in the concentration range investigated. Added SDS molecules can strongly associate with D40OCT30 aggregates because of the attractive hydrophobic and electrostatic interaction between SDS and the side groups of the polyelectrolyte. Careful examination of the titration curves, along with the turbidity and conductivity measurements, allowed the mapping of events that take place at varying polyelectrolyte/surfactant ratios. A model for the interaction is therefore proposed. Some important thermodynamic data, such as the $CAC_{complex}$ values, the $\Delta H_{total\ int}$, and phase boundaries have been derived from the observed enthalpy curves, which give more insight into the mechanism of interaction between the polyelectrolyte and the surfactant. An extension of this work is in progress, where we are investigating the effect of changing the length of the hydrophobic alkyl chains of the surfactant and the polyelectrolyte on the interaction of the mixed system.

Acknowledgment. We thank the FCT for financial support to CIQ(UP), Unidade de Investigação 81 for the project SAPIENS 35413/99 and for postdoctoral grants to G.B. and M.N. (Grants SFRH/BPD/5668/2001 and SFRH/BPD/5695/2001).

References and Notes

(1) Lindman, B.; Thalberg, K. In *Interactions of Surfactants with Polymers and Proteins*; Goddard, E. D., Ananthapadmanabhan, K. P., Eds.; CRC Press: Boca Raton, FL, 1993.

(2) Evans, D. F.; Wennerström, H. *The Colloidal Domain where Physics, Chemistry, Biology, and Technology Meet*; VCH Publisher: New York, 1994.

(3) Jönsson, B.; Lindman, B.; Holmberg, K.; Kronberg B. *Surfactants and Polymers in Aqueous Solution*; John Wiley & Sons Ltd: West Sussex, U.K., 1998.

(4) Iliopoulos, I. *Curr. Opin. Colloid Interface Sci.* **1998**, *3*, 493.

(5) Chu, D.; Thomas, J. K. *J. Am. Chem. Soc.* **1986**, *108*, 6270.

(6) Khokhlov, A. R.; Kramarenko, E. Yu.; Makhaeva, E. E.; Starodubtzev, S. G. *Macromolecules* **1992**, *25*, 4779.

(7) Yeh, F.; Sokolov, E. L.; Khokhlov, A. R.; Chu, B. *J. Am. Chem. Soc.* **1996**, *118*, 6615.

(8) Yeh, F.; Sokolov, E. L.; Walter, T.; Chu, B. *Langmuir* **1998**, *14*, 4350.

(9) Winnik, M. A.; Bystryak, S. M.; Chassenieux, C.; Strashko, V.; Macdonald, P. M.; Siddiqui, J. *Langmuir* **2000**, *16*, 4495.

(10) Bromberg, L.; Temchenko, M.; Colby, R. H. *Langmuir* **2000**, *16*, 2609.

(11) Li, Y.; Xu, R.; Couderc, S.; Bloor, D. M.; Warr, J.; Penfold, J.; Holzwarth, J. F.; Wyn-Jones, E. *Langmuir* **2001**, *17*, 5657.

(12) Nisha, C. K.; Basak, P.; Manorama, S. V.; Maiti, S.; Jayachandran, K. N. *Langmuir* **2003**, *19*, 2947.

(13) Guillemet, F.; Piculell, L. *J. Phys. Chem. B* **1995**, *99*, 9201.

(14) Thalberg, K.; van Stam, J.; Lindblad, C.; Almgren, M.; Lindman, B. *J. Phys. Chem.* **1991**, *95*, 8975.

(15) Thalberg, K.; Lindman, B.; Karlström, G. *J. Phys. Chem.* **1990**, *94*, 4289.

(16) Thalberg, K.; Lindman, B.; Karlström, G. *J. Phys. Chem.* **1991**, *95*, 6004.

(17) Magny, B.; Iliopoulos, I.; Zana, R.; Audebert, R. *Langmuir* **1994**, *10*, 3180.

(18) Svensson, A.; Piculell, L.; Cabane, B.; Ilekti, P. *J. Phys. Chem. B* **2002**, *106*, 1013.

(19) Li, Y.; Dubin P. L.; Havel, H. A.; Edwards, S. L.; Dautzenberg, H. *Macromolecules* **1995**, *11*, 2468.
(20) Hansson, P.; Schneider, S.; Lindman, B. *J. Phys. Chem. B* **2002**, *106*, 9777.
(21) Sokolov, E.; Yeh, F.; Khokhlov, A.; Grinberg, V. Y.; Chu, B. *J. Phys. Chem. B* **1998**, *102*, 7091.
(22) Li, Y.; Dubin P. L.; Dautzenberg, H.; Lück, U.; Hartmann, J.; Tuzar, Z. *Macromolecules* **1995**, *28*, 6795.
(23) Wang, Y. L.; Kimura, K.; Dubin, P. L.; Jaeger, W. *Macromolecules* **2000**, *33*, 3324.
(24) Li, Y.; Dubin P. L.; Havel, H. A.; Edwards, S. L.; Dautzenberg, H. *Macromolecules* **1995**, *28*, 3098.
(25) Li, Y.; Xia J.; Dubin P. L. *Macromolecules* **1994**, *27*, 7049.
(26) Xia, J. L.; Zhang, H. W.; Rigsbee, D. R.; Dubin, P. L.; Shaikh, T. *Macromolecules* **1993**, *26*, 2759.
(27) Semchyschyn, D. J.; Carbone, M. A.; Macdonald, P. M. *Langmuir* **1996**, *12*, 253.
(28) Claesson, P. M.; Fielden, M. L.; Dedinaite, A.; Brown, W.; Fundin, J. *J. Phys. Chem. B* **1998**, *102*, 1270.
(29) Fielden, M. L.; Claesson, P. M.; Schillen, K. *Langmuir* **1998**, *14*, 5366.
(30) Ilekti, P.; Martin, T.; Cabane, B.; Piculell, L. *J. Phys. Chem. B* **1999**, *103*, 9831.
(31) Windsor, R.; Neivandt, D. J.; Davies, P. B. *Langmuir* **2001**, *17*, 7306.
(32) Cooke, D. J.; Dong, C. C.; Thomas, R. K.; Howe, A. M.; Simister, E. A.; Penfold, J. *Langmuir* **2000**, *16*, 6546.
(33) Taylor, D. J. F.; Thomas, R. K.; Hines, J. D.; Humphreys, K.; Penfold, J. *Langmuir* **2002**, *18*, 9783.
(34) Mészáros, R.; Thompson, L.; Bos, M.; Varga, I.; Gilányi, T. *Langmuir* **2003**, *19*, 609.
(35) Artyukhin, A. B.; Burnham, K. J.; Levchenko, A. A.; Talroze, R. V.; Stroeve, P. *Langmuir* **2003**, *19*, 2243.
(36) Iliopoulos, I.; Furo, I. *Langmuir* **2001**, *17*, 8049.
(37) Iliopoulos, I.; Wang, T. K.; Audebert, R. *Langmuir* **1991**, *7*, 617.
(38) Bloor, D. M.; Holzwarth, J. F.; Wyn-Jones, E. *Langmuir* **1995**, *11*, 2312.
(39) Olofsson, G.; Wang, G. *Pure Appl. Chem.* **1994**, *3*, 527.
(40) Silva, R. C.; Olofsson, G.; Schillén, K.; Loh, W. *J. Phys. Chem. B* **2002**, *106*, 1239.
(41) Bai, G.; Wang, Y.; Yan, H.; Thomas, R. K.; Kwak, J. C. T. *J. Phys. Chem. B* **2002**, *106*, 2153.
(42) Dai, S.; Tam, K. C. *J. Phys. Chem. B* **2001**, *105*, 10759.
(43) Škerjanc, J.; Kogej, K.; Vesnaver, G. *J. Phys. Chem.* **1988**, *92*, 6382.
(44) Briggner, L.-E.; Wadsö, I. *J. Biochem. Biophys. Methods* **1991**, *22*, 101.
(45) Bastos, M.; Hägg, S.; Lönnbro, P.; Wadsö, I. *J. Biochem. Biophys. Methods* **1991**, *23*, 155.
(46) Santos, Luís M. N. B. F. Ph.D. Thesis, University of Porto, 1995.
(47) Wang, G.; Olofsson, G. *J. Phys. Chem.* **1995**, *99*, 5588.
(48) Bordi, E.; Colby, R. H.; Cametti, C.; De Lorenzo, L. Gili, T. *J. Phys. Chem. B* **2002**, *106*, 6887.
(49) Raju, B. B.; Winnik, F. M.; Morishima, Y. *Langmuir* **2001**, *17*, 4416.
(50) Bai, G.; Wang, Y.; Wang, J.; Han, B.; Yan, H. *Langmuir* **2001**, *17*, 3522.